Nuclear Instruments and Methods in Physics Research A ∎ (∎∎∎∎) ∎∎∎–∎∎∎

Contents lists available at ScienceDirect

Nuclear Instruments and Methods in Physics Research A

journal homepage: www.elsevier.com/locate/nima

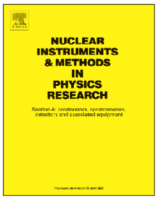

Surface effects in segmented silicon sensors

J. Schwandt*, E. Fretwurst, E. Garutti, R. Klanner, I. Kopsalis

Institute for Experimental Physics, University of Hamburg, Luruper Chaussee 147, D 22761, Hamburg, Germany

ARTICLE INFO

Article history:
Received 22 March 2016
Accepted 8 June 2016

Keywords:
Silicon sensors
Radiation damage
TCAD simulations
Oxide charges
Border traps
Interface traps

ABSTRACT

The voltage stability, charge-collection properties and dark current of segmented silicon sensors are influenced by the charge and potential distributions on the sensor surface, the charge distribution in the oxide and passivation layers, and by Si–SiO$_2$ interface states. To better understand these phenomena, measurements on test structures and sensors before and after X-ray irradiation, and TCAD simulations including surface and interface effects are performed at the Hamburg Detector Lab. The main results of these investigations and ongoing studies are presented.

1. Introduction

The breakdown behaviour, dark current and charge collection efficiency of segmented silicon sensors depends on the properties of the insulating layers, and the electric boundary conditions on the sensor surface. The phenomena are complex and depend on many parameters, which are influenced by radiation damage. In this paper methods are presented, how several of these parameters can be measured and implemented in TCAD simulations. Examples are given of the successful optimisation of a pixel sensor for X-ray doses up to 1 GGy and of the explanation of the dose- and humidity dependent charge collection efficiency observed for a silicon strip sensor. They demonstrate that TCAD simulations with realistic parameters can explain surprising observations and avoid design mistakes. Finally, work in progress on the field and voltage dependence of parameters characterising surface radiation damage is reported.

2. Surface parameters and TCAD simulations

2.1. Parameters for TCAD simulations

The parameters, relevant for surface effects, and the electrical boundary conditions for simulations, are presented in Fig. 1, which shows the cross section of a $p^{+}n$ strip sensor. These are:

1. The outer-surface charge density, Q_{os}, which can exhibit a time dependence, if the outer-surface resistivity is high.
2. The oxide-charge density, Q_{ox}, which depends on technology, crystal orientation, dose of ionising radiation, and the electric field during irradiation.
3. The border-trap charge density, Q_{border}, which depends on technology and ionising dose. Border traps are located in the SiO$_2$ within a few nm of the Si–SiO$_2$ interface and exchange charges with the Si with time constants, which can be seconds and even longer.
4. The charged Si–SiO$_2$ interface trap density, Q_{it}, which depends on technology, ionising dose and the Fermi energy at the interface.
5. The electrical boundary conditions: Bias voltage at the back side, ground potential on a plane at 0.2 mm distance parallel to the sensor surface (solid line), and Neumann conditions at the boundaries connecting the centres of the strips with the back plane (dashed lines).

We note that the charge densities depend on position, if the electric field during irradiation or operation is not uniform. So far in the simulations uniform charge densities have been assumed.

In previous studies on high-ohmic detector-grade Si [1] C–V measurements on MOS capacitors from four vendors have been used to determine the effective oxide charge density $N_{ox}^{eff} = (Q_{ox} + Q_{border} + Q_{it})/q_0$ for ionisation doses up to 1 GGy (elementary charge q_0). It has been found that before irradiation $N_{ox} \approx 10^{10}$ cm^{-2} for Si with ⟨100⟩ crystal orientation, and ≈10^{11} cm^{-2} for ⟨111⟩. For doses above 10–100 kGy, depending on the vendor, N_{ox} saturates between 1.5 and $3.5{\cdot}10^{12}$ cm^{-2}. In addition, the dose dependence of the surface generation current density, J_{surf}, which is related to Q_{it}, has been measured [2]. Before irradiation J_{surf} is a

---

* Corresponding author.
E-mail address: Joern.Schwandt@desy.de (J. Schwandt).

http://dx.doi.org/10.1016/j.nima.2016.06.032
0168-9002/© 2016 Elsevier B.V. All rights reserved.

Please cite this article as: J. Schwandt, et al., Nuclear Instruments & Methods in Physics Research A (2016), http://dx.doi.org/10.1016/j.nima.2016.06.032

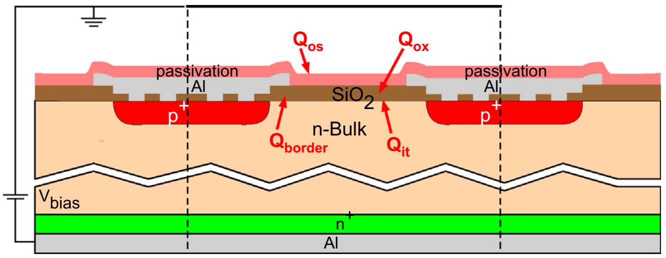

Fig. 1. Cross section of a strip sensor explaining the parameters relevant for surface effects.

few nA/cm^2, increases to ≈6 μA/cm^2 at a dose of about 10 MGy, and then decreases.

3. Impact of surface effects on sensors

3.1. Oxide charge and breakdown voltage

The AGIPD sensor [3] is an example for the successful optimisation of a 500 μm thick p^+n pixel sensor for X-ray doses up to 1 GGy at high operating voltages [4]. Fig. 2 left shows the voltage dependence of the current measured in the current-collection ring, which surrounds the pixels, for X-ray doses between 0 and 100 MGy for a sensor produced by SINTEF with standard technology: The breakdown voltage decreases from about 900 V to about 220 V. TCAD simulations explain the cause: For high oxide charges and the standard SiO$_2$ thickness of 700 nm, there is a single narrow high-field peak at the corner of the implantation. Reducing the oxide thickness to 250 nm results in two field peaks: One at the corner of the implantation and one below the edge of the metal overlap. As a result, the predicted breakdown voltage for $N_{ox} = 3\cdot10^{12}$ cm^{-2} exceeds 1000 V. The sensor has been produced with the optimised SiO$_2$ thickness of 250 nm, and Fig. 2 right shows that the breakdown voltage exceeds 900 V [4]. The increase in current for the non-irradiated sensor at 800 V is due to the depletion region reaching the cut edge. It disappears once the sensor has been exposed to a dose of a few 100 Gy, and thus does not present a problem. The observed current is dominated by the surface generation current and is correctly predicted using the surface-generation current density measured using Gate-Controlled-Diodes.

3.2. Outer-surface resistivity and charge collection

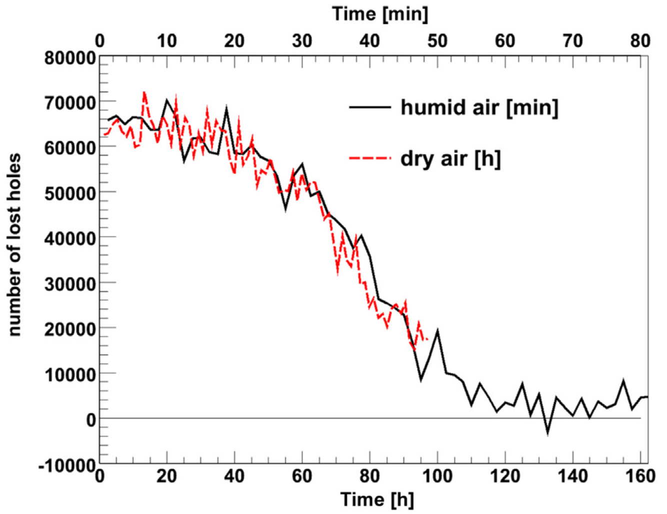

Fig. 3. Number of "lost" holes versus time for a p^+n Si strip sensor illuminated with 670 nm light, after changing the bias voltage from 500 to 200 V for relative humidities of 78% and <1%.

In Ref. [5] it is reported that, after changing the bias voltage, the charge collection of Si strip sensors changes with times constants, which depend on the relative humidity, *RH*. Fig. 3 shows an example. The voltage on a p^+n Si strip sensor was changed from 500 V to 200 V, and the charge collection for *eh* pairs, produced by laser light of 670 nm wavelength injected in-between the readout strips, has been measured at 20 °C and $RH \approx 78\%$ and <1%. At 670 nm the light-attenuation length in Si is about 3 μm, and the charge collection is sensitive to the electric field close to the Si–SiO$_2$ interface. In the figure the time dependence of the number of holes "lost", i.e. not recorded as signal in the readout strips within 50 ns, is shown. The time scale on top in minutes is for $RH = 78$ %, and the one at the bottom in hours for $RH < 1\%$. The shape of the curves are similar, however the time constants differ by a factor ≈120.

In order to understand this effect, we first have determined the outer-surface resistivity using the circular Gate-Controlled-Diode (GCD) described in Ref. [2], irradiated by X-rays to a dose of 1 GGy. Fig. 4 left shows $I_{GCD}(V_{gate})$, the current–voltage characteristics, when changing the gate voltage from inversion via depletion to accumulation. The current-peak is due to the surface-generation current, I_{surf}, from the radiation-damaged Si–SiO$_2$ interface. Then the GCD was biased in inversion, the gate contact disconnected and the time dependence $I_{GCD}(t)$ measured for *RH* values between 30 and 46%. Using $I_{GCD}(V_{gate})$, we derive $V_{gate}(t)$, shown in Fig. 4 right. An exponential dependence is found with time constants

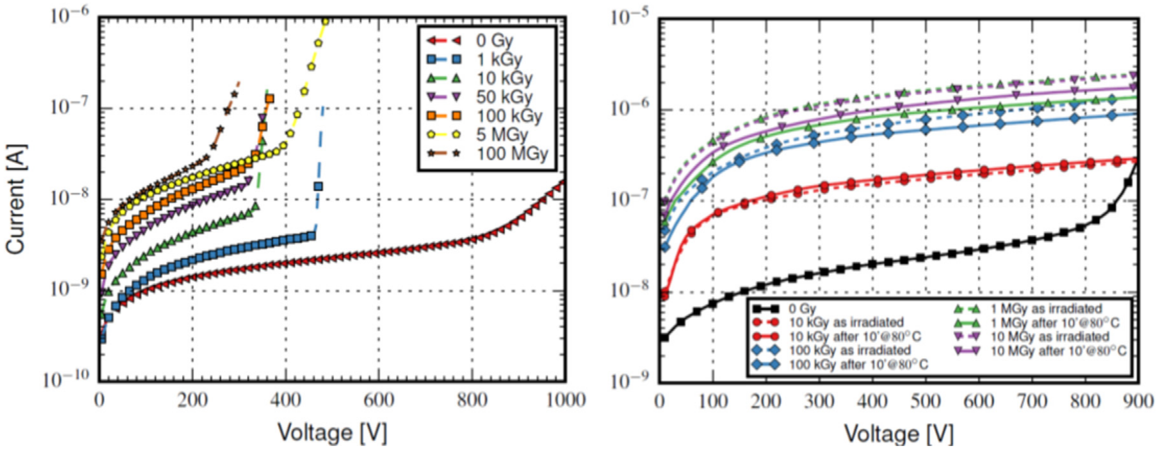

Fig. 2. Current–voltage characteristics for the current collection ring of a pixel sensor for different X-ray doses. Left standard, right optimised SINTEF technology.

Please cite this article as: J. Schwandt, et al., Nuclear Instruments & Methods in Physics Research A (2016), http://dx.doi.org/10.1016/j.nima.2016.06.032